water

MDPI

Article

Rapid Antibiotic Adsorption from Water Using MCM-41-Based Material

Jie Chen [1,†], Yao Yang [2,†], Yuanyuan Yao [1], Zhujian Huang [2], Qiaoling Xu [2], Liping He [1] and Beini Gong [2,*]

[1] CCCC Fourth Harbor Engineering Institute Co., Ltd., Guangzhou 510230, China; cjie12@cccc4.com (J.C.); yyuanyuan@cccc4.com (Y.Y.); e001@cccc4.com (L.H.)
[2] Guangdong Provincial Key Laboratory of Agricultural & Rural Pollution Abatement and Environmental Safety, College of Natural Resources and Environment, South China Agricultural University, Guangzhou 510642, China; yangyao@stu.scau.edu.cn (Y.Y.); zjhuang@scau.edu.cn (Z.H.); amy.198510@163.com (Q.X.)
* Correspondence: bngong@scau.edu.cn; Tel.: +86-13632245773
† These authors contributed equally to this work and should be considered co-first authors.

Abstract: The contamination of antibiotics in the environment has raised serious concerns, impacting both human life and ecosystems. This has led to a growing focus on the development of cost-effective and environmentally friendly adsorbent materials. Mesoporous molecular sieve MCM-41, known for its strong adsorption capacity, low cost, and efficient regenerative properties, holds significant promise for addressing this issue. In this study, we investigated the adsorption behavior of demolded MCM-41 materials in relation to tetracycline, doxycycline, and levofloxacin at different temperatures and pH levels. Our experiments encompassed the adsorption of these three common antibiotics, revealing that a neutral or weakly acidic pH environment promoted adsorption, whereas alkaline conditions hindered it. Utilizing the equilibrium isotherm model, we determined the theoretical maximum adsorption capacities for tetracycline (TC), doxycycline (DOX), and levofloxacin (LFX) as 73.41, 144.83, and 33.67 mg g^{-1}, respectively. These findings underscore the significant potential of MCM-41 in mitigating antibiotic wastewater contamination.

Keywords: MCM-41; antibiotics; rapidly adsorption; wastewater

Citation: Chen, J.; Yang, Y.; Yao, Y.; Huang, Z.; Xu, Q.; He, L.; Gong, B. Rapid Antibiotic Adsorption from Water Using MCM-41-Based Material. *Water* **2023**, *15*, 4027. https://doi.org/10.3390/w15224027

Academic Editors: Peiyue Li and Jianhua Wu

Received: 21 September 2023
Revised: 2 November 2023
Accepted: 6 November 2023
Published: 20 November 2023

1. Introduction

As urbanization progresses, the transformation of people's lifestyles and production methods is introducing new challenges. Consequently, the prevalence of emerging contaminants like antibiotics and dyes in water sources has surged. This surge in pollutants directly contributes to the degradation of water quality, impeding its recovery and efficient utilization. Simultaneously, antibiotic pollution exerts a profoundly detrimental impact on ecosystems, including animals, plants, and human populations. Notably, antibiotics like doxycycline (DOX), tetracycline (TC), and levofloxacin (LFX) have emerged as environmental pollutants, posing threats to diverse life forms [1]. Furthermore, the unregulated discharge of pollutants such as pharmaceutical waste, dyes, and heavy metals directly into water bodies, devoid of proper classification and pretreatment, represents a significant global environmental challenge within the context of sewage treatment [2].

Antibiotics are widely used to prevent and treat diseases and supplement animal feed. Presently, there are more than 20 types of tetracyclines. However, tetracycline (TC), chlortetracycline, oxytetracycline, and doxycycline (DOX) are the most commonly used antibiotics in the poultry industry [3]. Tetracyclines are used for disease treatment and prevention and as growth promoters for entire populations. Therefore, they deserve special attention due to their crucial role in health and the environment. Tetracycline (TC) is an antibiotic that humans and veterinarians use against various harmful bacteria. Maintaining activity after poor intestinal absorption will lead to residues in edible products. These residues

cause problems with the emergence and spread of antibiotic-resistant bacteria. DOX is also an antibiotic belonging to the tetracycline family, widely used in human and animal health. It has effectively treated infections in the human gut, kidneys, lungs, respiratory, and reproductive organs [4]. It is also used as an animal veterinary antibiotic [5]. Commonly used medical antibiotics include doxycycline, tetracycline, and levofloxacin [6]. They enter the environment through animal diets. In the body, they are usually not completely absorbed and metabolized. Between 30% and 90% of them can be discharged and released into the environment through animal excretion [7,8]. In addition to biological sources, antibiotics also come from wastewater in chemical manufacturing, mining, pharmaceutical, textile, and other industries. As a result, it contains high levels of toxic substances, organic pollutants, and many other complex compounds that destroy the integrity of the surface and groundwater [9–11]. These pollutants often are antibiotics such as levofloxacin and dyes such as Congo red, which may accumulate in the environment [12]. The wastewater treatment plant cannot completely remove antibiotics because they are non-biodegradable, thereby possessing a stable chemical structure. Then, the polluted wastewater flows into surface water, seeps into groundwater, and eventually into drinking water, which endangers the environment [13,14]. There are no standardized criteria for safe levels of antibiotic residues. However, in general, for some antibiotics that are difficult to degrade (e.g., tetracyclines), the residue level should not exceed 100 ng/L, and the total residue level of all types of antibiotics should not exceed 500 mg/L [15]. Current methods for removing organic compounds such as antibiotics include electrocoagulation [16], photocatalysis, chemical degradation, advanced oxidation, adsorption, solidification, membrane coagulation, ion exchange, reverse osmosis, and bioremediation [17–21]. Adsorption has been proven to be a feasible and economical method to remove water pollutants such as antibiotics and dyes. This prevalent research method has several advantages, including simpleness, fast kinetics, low cost, and high efficiency [22]. Various materials like clay minerals, activated carbon, zeolites, silica gels, polymeric resins, bioadsorbents, etc. can be used as adsorbents. The mechanism involves the adsorbents removing the target pollutants from the aqueous solution. Studies have shown adsorption can effectively reduce the emissions of antibiotics and organic contaminants in wastewater. The adsorption method has been widely used in wastewater treatment [12].

A molecular sieve is a new type of selective adsorbent medium with a high adsorption rate, which can selectively adsorb unsaturated, polar, and polarizable molecules according to molecular size and configuration. Common molecular sieve materials include zeolites, aluminophosphates, metal–organic frameworks, etc. The open framework structure and large internal and external specific surface area of mesoporous molecular sieve materials make them demonstrate unique adsorption functions [23]. At the same time, the molecular sieve has an excellent regeneration function because of its good physical and chemical stability. Mesoporous molecular sieve MCM-41 is a new synthetic molecular sieve with a regular hexagonal arrangement and uniform pore size. Studies have shown that MCM-41 has rich pore channels and good adsorption capacity. Also, MCM-41 has the advantages of low cost, strong adsorbent regeneration, and high application value. Presently, the research on mesoporous material MCM-41 mostly stays in the adsorption of antibiotic pollutants after modification. In contrast, the adsorption research on MCM-41 without modification mostly focuses on dye organics. Up to now, the adsorption of antibiotic pollutants has not been reported.

Previous studies have demonstrated the advantages of using MCM-41 as an adsorbent for antibiotic pollutants. In this study, we explore the adsorption performance of these demolded MCM-41 materials concerning three different pollutants across varying temperatures. Factors such as adsorption duration, MCM-41 surface charge, and the underlying physical properties of the adsorption mechanism are meticulously examined and confirmed. Utilizing adsorption kinetics and isotherm models, we assess the adsorption data for these three distinct pollutants, providing valuable insights into the adsorption mechanism's

intricacies. The zeta potential characterization of MCM-41 materials serves as a pivotal tool in enhancing our understanding of the adsorption process and its associated mechanisms.

2. Materials and Methods

2.1. Materials

The analytical reagents employed in this study consisted of MCM-41, tetracycline (C22H24N2O8•HCl), sodium hydroxide (NaOH), levofloxacin, doxycycline, and hydrochloric acid. Initially, the MCM-41 molecular sieve was procured from Tianjin Yuanli Chemical Co., Ltd. (Tianjin, China). Subsequently, tetracycline, levofloxacin, and doxycycline antibiotics were obtained from Shanghai Yuanye Biotechnology Co., Ltd. (Shanghai, China). Hydrochloric acid (HCL) and sodium hydroxide (NaOH) were purchased from Sinopharm Chemical Reagent Co. (Shanghai, China). Moreover, ultrapure water served as the primary solvent throughout the experimental procedures.

2.2. Mesoporous MCM-41 Demolding Treatment

The acquired full-silica MCM-41 molecular sieve was loaded into a ceramic crucible weighing 4.0 g. The crucible, containing the molecular sieve, was then placed inside a box furnace. in the demolded samples were calcined at the temperature of 550 °C, 600 °C, 700 °C, 800 °C and 900 °C, respectively. Following this temperature ramp-up sequence, a constant temperature was maintained for a duration of six hours. Subsequently, the contents were allowed to cool, and the materials were packed into bags.

2.3. Adsorption Experiments on Three Kinds of Pollutants

Approximately 0.06 g of tetracycline was dissolved in a beaker and subsequently transferred to a 2-L volumetric flask, resulting in a tetracycline solution with a concentration of 30 mg/L. Simultaneously, a 10 mL centrifuge tube was prepared to hold the sample. In a separate 800 mL beaker equipped with a 250 mL measuring tube, approximately 200 mL of the tetracycline solution was added. The solution was then subjected to constant temperature magnetic stirring. The stirring parameters were initially set to 200 r/min with synchronous operations. Furthermore, six distinct beakers, each labeled as 550, 600, 700, 800, 900, and a blank control, were loaded with 0.1 g of MCM-41 calcined at temperatures of 550 °C, 600 °C, 700 °C, 800 °C, and 900 °C, respectively. These mixtures were stirred with 8 mL of sampling liquid in a 10 mL centrifuge tube for varying durations, specifically 10 min, 20 min, 30 min, 40 min, 70 min, 100 min, and 130 min, using a disposable syringe for uniform distribution. Subsequently, the absorbance values were measured at wavelengths of 375 nm, 351 nm, and 287 nm using a UV spectrophotometer to determine the concentrations of tetracycline, doxycycline, and levofloxacin, respectively.

The adsorption isotherms for three antibiotics adsorption by MCM-41 mesoporous materials were modelled using the Freundlich, Langmuir, and Temkin equations.

$$\text{Freundlich isotherm:} \qquad Q_e = K_F {C_e}^n \tag{1}$$

where Q_e equals the amount of adsorption, and K_F is the Freundlich adsorption coefficient, relating to the capacity and the intensity of adsorption. C_e is the equilibrium concentration of three antibiotics in the solution. n is Freundlich adsorption index.

$$\text{Langmuir isotherm}: \quad Q_e = \frac{Q_m K_L C_e}{1 + K_L C_e} \tag{2}$$

where Q_m is the limited monolayer adsorption capacity. K_L is the Langmuir adsorption coefficient representing the affinity of the adsorbent for the adsorbate.

$$\text{Temkin isotherm}: \quad Q_e = \left(\frac{RT}{b_T}\right)\ln A_T + \left(\frac{RT}{b_T}\right)\ln C_e \tag{3}$$

where b_T is Temkin heat of adsorption, and A_T is the Temkin adsorption potential.

A series of adsorption experiments using solutions containing tetracycline, doxycycline, and levofloxacin at varying initial concentrations were conducted: 0 mg·L^{-1}, 10 mg·L^{-1}, 15 mg·L^{-1}, 20 mg·L^{-1}, 25 mg·L^{-1}, 30 mg·L^{-1}, 35 mg·L^{-1}, 40 mg·L^{-1}, and 50 mg·L^{-1}. These experiments were designed to establish a correlation between the initial concentration of the solutions and the adsorption capacity. Consequently, we aimed to assess how the initial concentration influences the adsorption capacity of the mesoporous material MCM-41.

About 0.05 g of tetracycline, doxycycline, and levofloxacin were dissolved in 1 L volumetric flask. The concentration of pollutants was 50 mg·L^{-1}. Different solutions of 0 mL, 4 mL, 6 mL, 8 mL, 10 mL, 12 mL, 14 mL, 16 mL, and 20 mL were put into nine 50 mL beakers using a 25 mL measuring tube. Then, a certain amount of distilled water was added to the 20 mL solution. Approximately 0.1 g MCM-41 adsorbent calcined at 800°was added to the solution and filtered using a 0.45 μm filter. Subsequently, the absorbance value was determined.

At room temperature, adsorption experiments were conducted using 50 mg·L^{-1} solutions of tetracycline, doxycycline, and levofloxacin. The aim was to assess the adsorption kinetics at various time intervals and ascertain the point of adsorption equilibrium. Each group consisted of three parallel experiments. To initiate the experiments, 200 mL of the pollutant solution was poured into a 500 mL beaker. Subsequently, 0.1 g of mesoporous material MCM-41 was introduced into the beaker, and the solution was placed on a magnetic stirrer. The stirring commenced at a predetermined time, maintaining a constant rotational speed of 250 r/min. Stirring intervals included 0 min, 1 min, 2 min, 3 min, 4 min, 5 min, 7 min, 9 min, 20 min, 30 min, 40 min, 50 min, 60 min, and 70 min. Following the designated stirring time, the solution underwent filtration using a 0.45 μm filter membrane. Subsequently, it was transferred into a centrifuge tube, and the pollutant concentrations in the solution were quantified using a spectrophotometer. The concentrations of pollutants remained stable after reaching adsorption equilibrium.

3. Results

3.1. Physicochemical Properties of MCM-41

As shown in Figure 1, different calcination temperatures had little effect on the adsorption performance of MCM-41 material, but the adsorption performance was significantly highest at 800 °C. As shown in Figure 2, the peak tends toward an increasing angle and then to a decreasing angle with an increase in the calcination demolding temperature. This shows that the empty surface structure of the material becomes smaller and larger. When the temperature is too high, many pores are melted, and the peak disappears. The X-ray diffraction (XRD) images for MCM-41 calcined within the temperature range of 550–800 °C closely resemble those of the original MCM-41, indicating the preservation of its ordered structure. However, a significant alteration in the image becomes apparent at the 900 °C calcination temperature. While the pure adsorption efficacy is optimal at 900 °C calcination, this temperature jeopardizes the integrity of the ordered mesoporous material structure. It is worth noting that the calcination process demands substantial energy consumption and prolonged durations, rendering it impractical for certain applications.MCM-41 has a strong peak at 2θ = 5.5° corresponding to the (100) of hexagonal mesoporous structure, of which the spacing distance is 1.589 nm. After 900 °C of calcination, the reflection (100) collapsed.

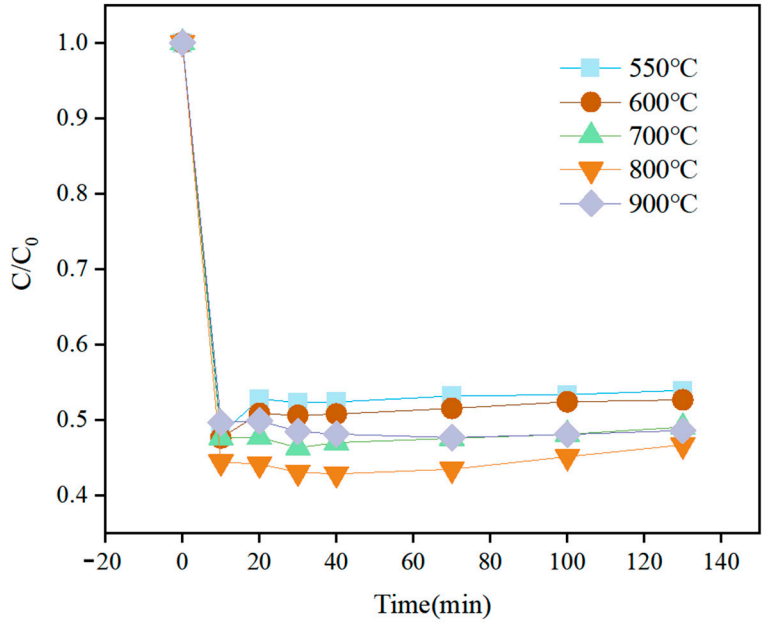

Figure 1. Comparison of adsorption performance on MCM-41 materials at different calcination temperatures (demold temperature: 550 °C, 600 °C, 700 °C, 800 °C, 900 °C; TC concentration: 30 mg/L; MCM-41 concentration: 0.5 g/L).

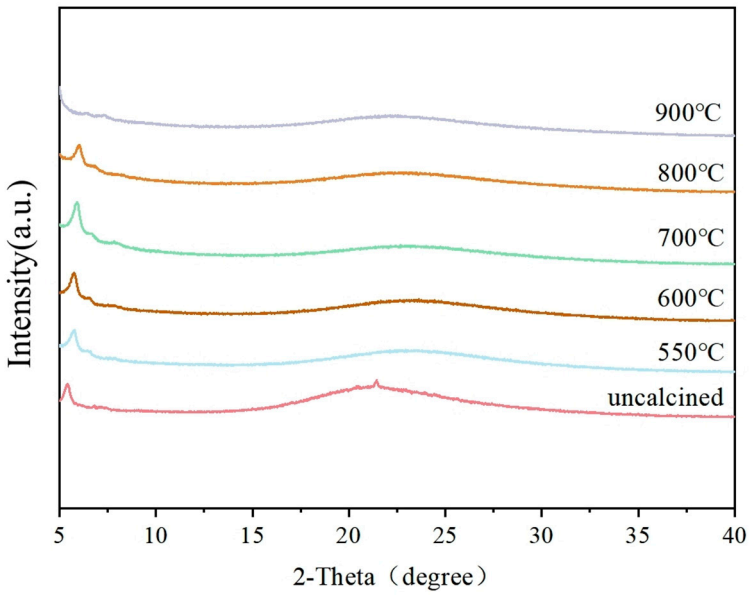

Figure 2. XRD patterns of MCM-41 materials at different calcination temperatures.

3.2. Adsorption of Antibiotics

Figure 3 illustrates the temporal evolution of pollutant adsorption by MCM-41, revealing a gradual increase in adsorption with time, culminating in a plateau at a specific time point. This plateau signifies that the available pollutants are retained in the solution, establishing a dynamic equilibrium between adsorbed and unadsorbed pollutants within the adsorbent. The duration required to attain this equilibrium state is referred to as the equilibrium time, and the quantity of pollutants adsorbed at this juncture represents the maximum adsorption capacity under these unique conditions. Remarkably, the equilibrium state is reached in less than 10 min, underscoring the rapid adsorption observed during the initial 10 min. This phenomenon can be attributed to the abundant availability of active sites on the surface of MCM-41. As these sites gradually become occupied, the efficiency of adsorption diminishes, and the rate of adsorption slows as it approaches equilibrium.

Prior research [24] has demonstrated that MCM-41 possesses a notably high saturated adsorption capacity. The generous pore size on the surface of MCM-41 allows pollutants to swiftly enter and undergo adsorption, leading to a mechanism characterized as continuous adsorption–diffusion–adsorption [25], where adsorption progresses from the exterior to the interior of the material.

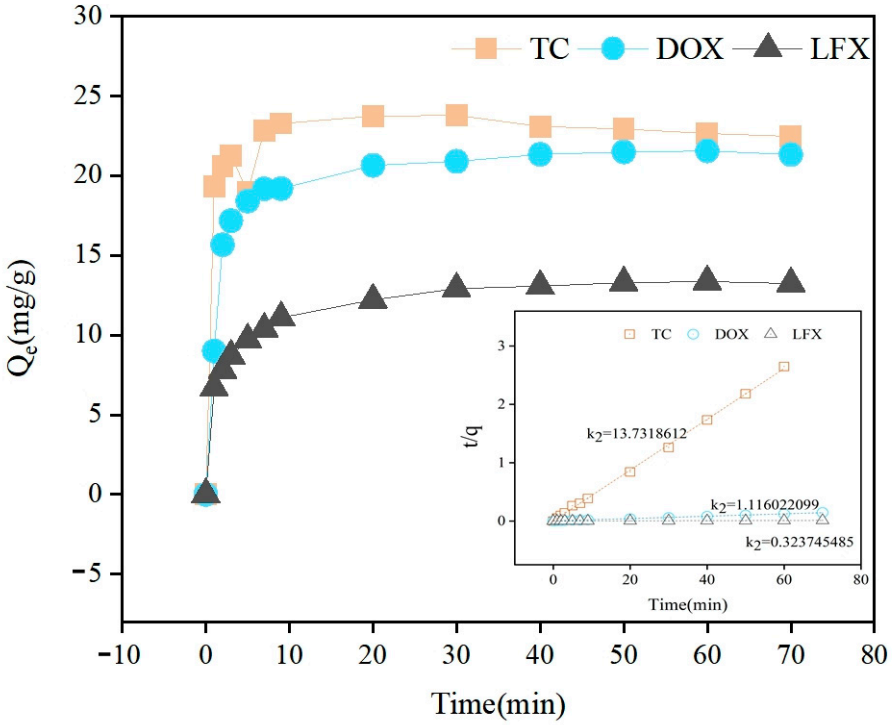

Figure 3. Adsorption effect of MCM-41 (800 °C) on different pollutants and kinetic equation of pseudo-second-order adsorption rate kinetic model diagram (initial TC, DOX, LFX concentration: 50 mg/L; adsorbent dose: 0.5 g/L; pH: 7.0; temperature: 25 °C).

The kinetic study of the adsorption process mainly describes the adsorbent's absorption rate, which controls the retention time of the adsorbent at solid–liquid interface. The adsorption kinetics model can be described using Lagrange's first-order rate equation:

$$\frac{dq}{dt} = k_1(q_e - q) \tag{4}$$

The Ho and McKay equation describes the pseudo-second-order model of adsorption kinetics. It is based on the rate control step. In addition, it is a second-order kinetic equation for chemical adsorption via chemical reactions involving the sharing, gaining, or losing of electrons. The expression formula of the second-order dynamic equation is as follows:

$$\frac{dq}{dt} = k_2(q_e - q)^2 \tag{5}$$

where mg/g is the equilibrium adsorption quantity, mg/g is the adsorption quantity for a certain time, min is the first-order adsorption kinetic rate constant, and g/(mg·min) is the second-order adsorption kinetic rate constant. For Formulas (4) and (5), from $t = 0$ to $t > 0$ (=0 to >0), the linear form is as follows:

$$\ln(q_e - q) = lnq_e - k_1 t \tag{6}$$

$$\frac{t}{q} = \frac{1}{k_2 q_e} + \frac{t}{q_e} \tag{7}$$

The adsorption experiments for tetracycline (TC), doxycycline (DOX), and levofloxacin (LFX) at a concentration of 50 mg/L were conducted under identical conditions, including stirring speed, temperature (25 °C), and MCM-41 concentration. Subsequently, the adsorption kinetics data obtained for MCM-41 were fitted to kinetic models, specifically the first-order and second-order kinetic adsorption models, as illustrated in Figure 3. The dynamic parameters resulting from the correlation calculations are presented in Table 1. The fitting outcomes reveal that the adsorption of TC, DOX, and LFX by MCM-41 conforms to the second-order adsorption kinetics model, as indicated by R2 values of 0.999. This observation suggests that the adsorption of these three pollutants by MCM-41 is characterized as chemical adsorption. Therefore, the adsorption of the three antibiotics onto MCM-41 demonstrated high efficiency, and this mode of adsorption can be attributed to chemical adsorption.

Table 1. Kinetic parameters for the adsorption of TC, DOX, and LFX onto MCM-41.

Pollutants	Adsorption Capacity Determined by Experiment qe, exp (mg/g)	Kinetic Equation of Pseudo-First-Order Adsorption Rate			Kinetic Equation of Pseudo-Second-Order Adsorption Rate		
		k_1	q_e	R^2	k_2	q_e	R^2
TC	23.77	0.02	2.30	0.126	13.73	22.97	0.999
DOX	21.54	0.06	6.39	0.843	1.12	495.04	0.998
LFX	13.35	0.06	0.93	0.941	0.32	6794.07	0.997

k_1: min, k_2: g/(mg·min), and q_e: mg/g.

The equilibrium relationship existing between MCM-41 and pollutants was described by the adsorption isotherms. The adsorption isotherms of mesoporous material MCM-41 for the three types of antibiotics are shown in Figure 4. The values of adsorption constants (K_F, n, K_L, Q_m, b_T, A_T, R^2) are shown in Table 2. The correction coefficient R^2 shows that the Langmuir model (0.96–0.99) can better describe the adsorption process than the Temkin model (0.95–0.98). This result showed that antibiotic adsorption on MCM-41 could be a multilayer. Therefore, it is concluded that the adsorption force of MCM-41 for these three types of pollutants is similar to the surface bond force forming a certain chemical bond. The obtained results are consistent with the second-order kinetic fitting results, which are related to the characteristics of MCM-41 and the adsorbed substances. MCM-41 provides a specific uniform site for the adsorption of pollutants [26,27]. According to the values of Q_m, K_L, and K_F, the maximum adsorption capacity and affinity of MCM-41 for these three antibiotics were in the order of TC > DOX > LFX. Therefore, it is speculated that MCM-41 has more adsorption capacity for tetracycline and doxycycline, composed of hydrocarbon elements. In contrast, it has a different adsorption capacity for levofloxacin not composed of hydrocarbon elements. It also shows that a single layer can control the whole adsorption process. These findings are consistent with the kinetic experiments.

Table 2. Equilibrium isotherm model parameters for TC, DOX, and LFX adsorption onto MCM-41 composites.

Pollutants	Freundlich			Langmuir			Temkin		
	K_F	n	R^2	K_L	Q_m	R^2	b_T	A_T	R^2
TC	12.89	0.33	0.95	0.204	73.410	0.96	373.01	8.90	0.96
DOX	13.39	0.27	0.99	0.100	144.835	0.99	809.60	532.80	0.95
LFX	18.93	0.13	0.81	1.47	33.676	0.98	456.52	12.89	0.98

K_F: L/g, K_L: L/μmol, b_T: kJ/mol, and A_T: L/mmol s.

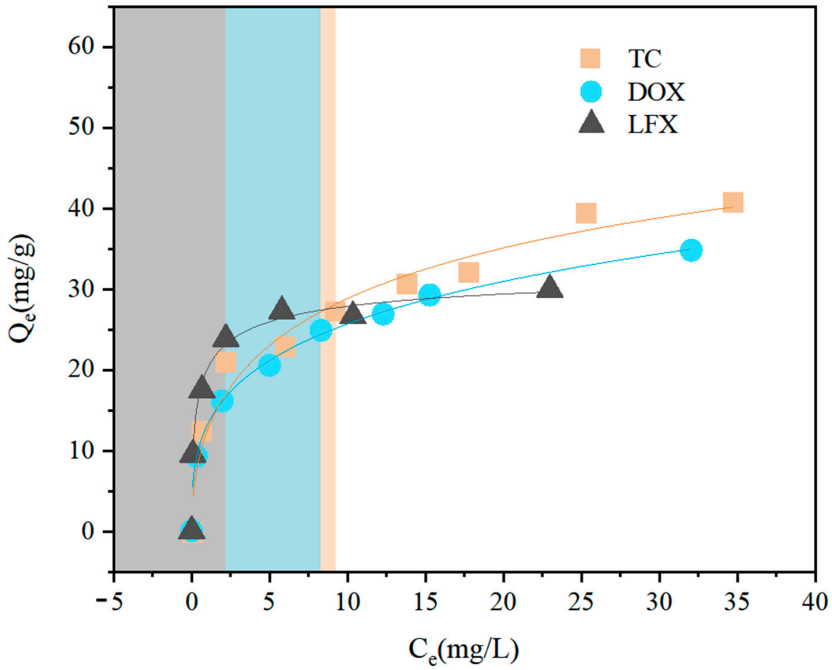

Figure 4. Langmuir isotherms of demolded MCM-41 at 800 °C for TC, DOX, and LFX. (pH: 7.0; adsorbent dosage: 0.5 g/L; temperature: 25 °C; contact time: 70 min).

The pH of a solution plays a pivotal role in influencing the adsorption capacity of mesoporous materials. However, it also has a bearing on the characteristics of the adsorbents and the charge state and presence of ions. In our study, we manipulated the pH value by employing hydrochloric acid and sodium hydroxide solutions. The objective was to investigate the adsorption behavior of the four different pollutants on mesoporous material MCM-41 under varying pH conditions. The pH values ranged from approximately 3 to 11, in conjunction with the zeta potential diagram of MCM-41 (Figure 5).

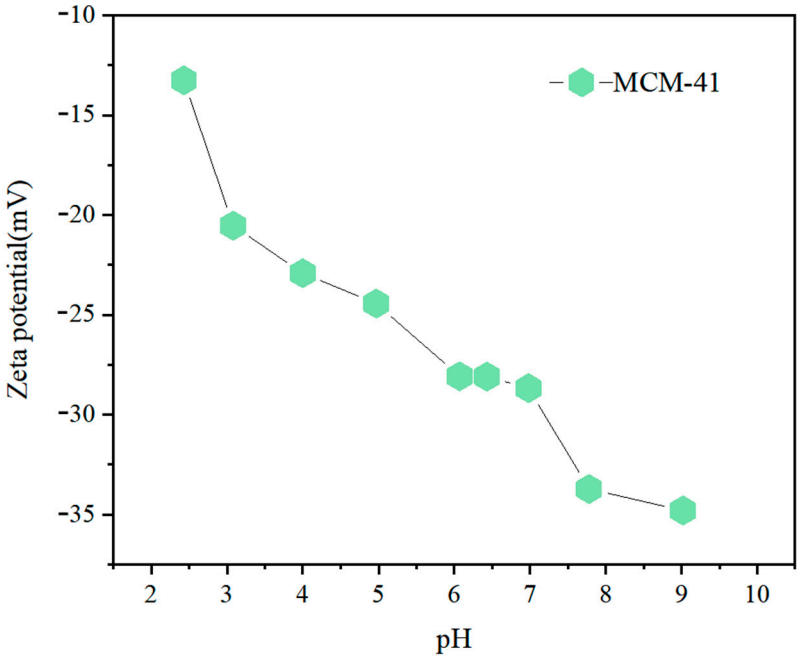

Figure 5. 800 °C MCM-41 Zeta potential diagram (pH: 7.0; adsorbent dosage: 0.5 g/L; temperature: 25 °C).

Regarding tetracycline (TC) adsorption (as shown in Figure 6), an impressive removal rate of 97.88% was achieved at a pH of 4. However, as the pH increased, the removal rate of TC exhibited a decline. The adsorption process typically involves several mechanisms, including electrostatic interactions, hydrogen bond formation, electron donor–acceptor interactions, and π-π dispersion interactions [28]. These phenomena are strongly influenced by pH values, consequently impacting the adsorption process. The underlying rationale for this behavior may be linked to the molecular structure of TC and the functional groups present on the surface of MCM-41. In aqueous solutions, TC comprises three distinct functional groups. Depending on the pH, these groups can undergo protonation or deprotonation reactions, rendering the TC molecule positively charged (under acidic conditions), neutrally charged (within the pH range of 4–8), or negatively charged (under alkaline conditions).

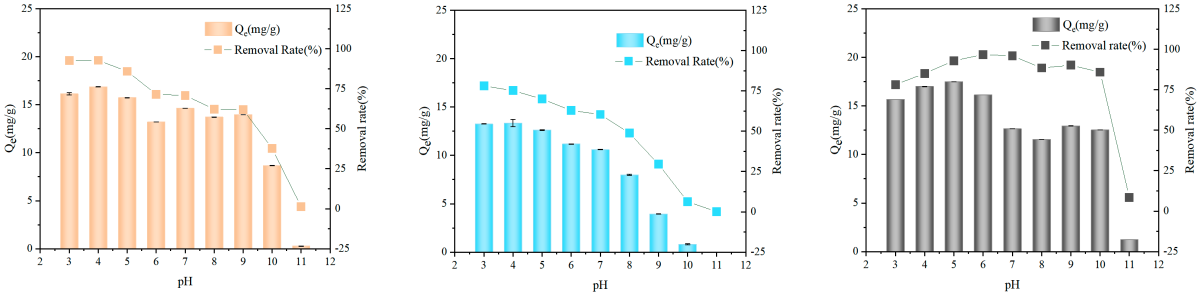

Figure 6. Effect of initial pH on adsorption of (**a**) TC, (**b**) DOX, and (**c**) LFX on MCM-41 (initial concentration: 10 mg/L; adsorbent dose: 0.5 g/L; temperature: 25 °C; contact time: 70 min).

When the pH is below the pKa value (7.78) of tetracycline (TC), TC molecules carry a positive charge, specifically as TCH3+ and TCH2± species. Conversely, at low pH values, MCM-41 also exhibits a positive charge [29]. As the pH increases, TC molecules acquire negative charges. Considering the properties of TC and the zeta potential diagram of MCM-41, it becomes evident that the zeta potential of the material decreases as the pH increases. This phenomenon indicates that the material becomes electronegative in an aqueous solution, resulting in a diminished electrostatic attraction between the surface charge of MCM-41 and TC, thereby reducing adsorption capacity. Consequently, both the adsorption rate and capacity decrease with increasing pH. Overall, the electrostatic repulsion between TC and MCM-41 is more pronounced under lower pH conditions, whereas higher pH levels intensify electrostatic negative repulsion. Furthermore, the pH-dependent adsorption behavior highlights that the MCM-41 adsorbent is capable of maintaining significant adsorption capacity over a broad range of low pH conditions.

For doxycycline (DOX) adsorption (as illustrated in Figure 6), the removal rate exhibited a decline as the pH increased. The highest removal rate, 78.1%, was achieved at pH 3, and it substantially decreased at pH 7. This suggests that DOX exhibits a pronounced affinity for MCM-41 at lower pH levels. The zeta potential and pH data further confirm that under the experimental conditions, the MCM-41 surface carried a negative charge, primarily due to pH-dependent variations in surface hydroxyl sites [30]. Consequently, the adsorption capacity of DOX decreased with rising pH. This phenomenon can be attributed to two key factors: (a) the increase in the number of negatively charged sites on the surface of MCM-41 due to the loss of H+ ions; (b) research has shown that DOX molecular species include DCH3+ (above pH 3.5, pKa1), DCH2± (above pH 7.7, pKa2), and DCH− (above pH 9.5, pKa3), with their charge states varying with pH.

As the pH level rises, doxycycline (DOX) undergoes deprotonation, resulting in a heightened net negative charge. These dual effects combine to increase the electrostatic repulsion between DOX and the adsorbent. It is important to note that aside from electrostatic interactions, the adsorption process also encompasses non-electrostatic interactions

between organic compounds and solid surfaces. These non-electrostatic interactions encompass phenomena like hydrogen bonding, surface complexation, and van der Waals forces, which can occur with cations (DCH3+) as well as DCH2± and DCH−, all of which can contribute to the adsorption process [31]. However, the significance of these contributions diminishes notably with increasing pH.

For LFX, the maximum removal rate reached 96.73% at pH = 6, close to pKa1 of LFX. Also, the removal rate decreased significantly at pH = 10. LFX molecule is the cation below pH = 6 (protonated piperazine, H2L+), anion above pH = 8.5 (deprotonated carboxyl, L−), and amphoteric ion at pH between pKa1 and pKa2 [25]. The morphology of LFX molecules at different pH levels greatly influences adsorption. In the range of pH 6.0–8.0, levofloxacin can undergo various acid-base equilibrium, forming anions, cations, and dipoles. LFX changes with pH. The formation of the protonated piperazine group and dissociation equilibrium of the carboxylic acid group occurred at a pH value close to pKa1 (pH = 6.02). However, the partial deprotonation of the pyrazinyl group occurred at pH near pKa2 (pH = 8.15).

When the pH falls below 6, levofloxacin (LFX) exhibits an increasing positive charge as pH decreases. In this pH range, LFX carries a positive charge, whereas MCM-41 surfaces bear a negative charge. Consequently, the adsorption rates between these two entities are notably high. The enhanced adsorption of LFX is a consequence of the intensified attraction between the protonated amine groups, whether they are adsorbed or free, present on the LFX molecule. This attraction is also influenced by the negatively charged surface of MCM-41. As the pH increases, the deprotonation of the pyrazine group in LFX diminishes the positive charge of LFX. This, in turn, hinders the adsorption of LFX onto MCM-41 and heightens the electrostatic repulsion between them, particularly at higher pH levels. As a result, the maximum adsorption of LFX occurs at pH = 6 (as depicted in Figure 6).

In the aqueous solution utilized in this study, the three distinct molecules underwent protonation and deprotonation reactions in response to changes in pH values. Consequently, they formed varying chemical species [32]. As the pH increased, the deprotonation process (pH > pKa) followed a particular order, typically involving the initial deprotonation, followed by the second deprotonation, and finally, the third deprotonation step. These deprotonation steps emanate from the surface charge characteristics of the pollutants and exert a discernible influence on the adsorption rate of the adsorbent, in accordance with the pKa values associated with each individual pollutant.

4. Conclusions

The adsorbent medium was prepared by demolding mesoporous material MCM-41 at elevated temperatures. This adsorbent medium proves to be a remarkably efficient and effective system for the removal of antibiotics in water, encompassing tetracycline, doxycycline, and levofloxacin. Consequently, it facilitates the purification of wastewater. The experimental findings unequivocally demonstrate that the adsorption efficiency for all three organic pollutants consistently exceeds 95%, and the maximum adsorption capacities for tetracycline (TC), doxycycline (DOX), and levofloxacin (LFX) were 73.41, 144.83, and 33.67 mg g^{-1}, respectively. The adsorption of these three organic pollutants by MCM-41 predominantly falls under the category of chemical adsorption. This multifaceted process involves chemical ion exchange, intraparticle diffusion, hydrogen bonding, and electrostatic interactions, it accounts for the excellent adsorption performance of MCM-41 and provides insights into designing highly efficient adsorbent materials. Furthermore, the results underscore the favorable impact of a neutral or weakly acidic pH on adsorption, while the presence of alkaline conditions inhibits adsorption, which can be directly applied in engineering design and represents the first quantitative result in this field. In summary, MCM-41 emerges as a highly efficient adsorbent characterized by a rapid adsorption rate and short adsorption time, rendering it suitable for use in a fluidized bed setup. Simultaneously, this material offers the advantages of being effective, environmentally

friendly, non-toxic, easily recoverable, and capable of selectively removing antibiotics and dye pollution from water.

Author Contributions: J.C. (first author): conceptualization, experiment, formal analysis, writing—original draft, software, and visualization. Y.Y. (Yao Yang) (co-first author): conceptualization, visualization, investigation, and writing—review and editing. Y.Y. (Yuanyuan Yao): investigation and writing—review and editing. Z.H.: conceptualization, funding acquisition, resources, supervision, and writing—review and editing. Y.Y. (Yuanyuan Yao): investigation and writing—review and editing. Q.X.: resources and supervision. L.H.: conceptualization, methodology, and supervision. B.G. (corresponding author): conceptualization, methodology, and supervision. All authors have read and agreed to the published version of the manuscript.

Funding: The study was supported by the Key-Area Research and Development Program of Guangdong Province (2020B0202080001), the Natural Science Foundation of Guangdong Province (2019A1515011659), and the National Natural Science Foundation of China (No. 51509093). The characterization results were supported by Beijing Zhongkebaice Technology Service Co., Ltd.

Data Availability Statement: All data employed in support of the outcomes of the study are included in this article.

Conflicts of Interest: Author Jie Chen, Yuanyuan Yao and Liping He was employed by the company CCCC Fourth Harbor Engineering Institute Co., Ltd. The remaining authors declare that the research was conducted in the absence of any commercial or financial relationships that could be construed as a potential conflict of interest.

References

1. Wang, J.; Xu, S.; Zhao, K.; Song, G.; Zhao, S.; Liu, R. Risk control of antibiotics, antibiotic resistance genes (ARGs) and antibiotic resistant bacteria (ARB) during sewage sludge treatment and disposal: A review. *Sci. Total Environ.* **2023**, *877*, 162772. [CrossRef]
2. Apreja, M.; Sharma, A.; Balda, S.; Kataria, K.; Capalash, N.; Sharma, P. Antibiotic residues in environment: Antimicrobial resistance development, ecological risks, and bioremediation. *Environ. Sci. Pollut. Res.* **2021**, *29*, 3355–3371. [CrossRef]
3. Kalli, M.; Noutsopoulos, C.; Mamais, D. The Fate and Occurrence of Antibiotic-Resistant Bacteria and Antibiotic Resistance Genes during Advanced Wastewater Treatment and Disinfection: A Review. *Water* **2023**, *15*, 2084. [CrossRef]
4. McClain, J.B.L.; Ballou, W.R.; Harrison, S.M.; Steinweg, D.L. Doxycycline therapy for leptospirosis. *Ann. Intern. Med.* **1984**, *100*, 696–698. [CrossRef]
5. Bhattacharyya, P.; Parmar, P.R.; Basak, S.; Dubey, K.K.; Sutradhar, S.; Bandyopadhyay, D.; Chakrabarti, S. Metal organic framework-derived recyclable magnetic coral Co@Co_3O_4/C for adsorptive removal of antibiotics from wastewater. *Environ. Sci. Pollut. Res.* **2023**, *30*, 50520–50536. [CrossRef] [PubMed]
6. Mohy-U-Din, N.; Farhan, M.; Wahid, A.; Ciric, L.; Sharif, F. Human health risk estimation of antibiotics transferred from wastewater and soil to crops. *Environ. Sci. Pollut. Res.* **2023**, *30*, 20601–20614. [CrossRef]
7. Zhou, C.-S.; Cao, G.-L.; Wu, X.-K.; Liu, B.-F.; Qi, Q.-Y.; Ma, W.-L. Removal of antibiotic resistant bacteria and genes by nanoscale zero-valent iron activated persulfate: Implication for the contribution of pH decrease. *J. Hazard. Mater.* **2023**, *452*, 131343. [CrossRef] [PubMed]
8. Ajduković, M.; Stevanović, G.; Marinović, S.; Mojović, Z.; Banković, P.; Radulović, K.; Jović-Jovičić, N. Ciprofloxacin Adsorption onto a Smectite-Chitosan-Derived Nanocomposite Obtained by Hydrothermal Synthesis. *Water* **2023**, *15*, 2608. [CrossRef]
9. Raper, E.; Stephenson, T.; Anderson, D.R.; Fisher, R.; Soares, A. Industrial wastewater treatment through bioaugmentation. *Process Saf. Environ. Prot.* **2018**, *118*, 178–187. [CrossRef]
10. Hasan, R.; Chong, C.; Setiabudi, H.; Jusoh, R.; Jalil, A. Process optimization of methylene blue adsorption onto eggshell-treated palm oil fuel ash. *Environ. Technol. Innov.* **2019**, *13*, 62–73. [CrossRef]
11. Gurgenidze, D.; Romanovski, V. The Pharmaceutical Pollution of Water Resources Using the Example of the Kura River (Tbilisi, Georgia). *Water* **2023**, *15*, 2574. [CrossRef]
12. Ighalo, J.O.; Adeniyi, A.G. Mitigation of Diclofenac Pollution in Aqueous Media by Adsorption. *ChemBioEng Rev.* **2020**, *7*, 50–64. [CrossRef]
13. Wang, X.; Yin, R.; Zeng, L.; Zhu, M. A review of graphene-based nanomaterials for removal of antibiotics from aqueous environments. *Environ. Pollut.* **2019**, *253*, 100–110. [CrossRef]
14. Lim, S.; Shi, J.L.; von Gunten, U.; McCurry, D.L. Ozonation of organic compounds in water and wastewater: A critical review. *Water Res.* **2022**, *213*, 118053. [CrossRef]
15. Madan, S.; Shaw, R.; Tiwari, S.; Tiwari, S.K. Adsorption dynamics of Congo red dye removal using ZnO functionalized high silica zeolitic particles. *Appl. Surf. Sci.* **2019**, *487*, 907–917. [CrossRef]
16. Zaidi, S.; Chaabane, T.; Sivasankar, V.; Darchen, A.; Maachi, R.; Msagati, T. Electro-coagulation coupled electro-flotation process: Feasible choice in doxycycline removal from pharmaceutical effluents. *Arab. J. Chem.* **2019**, *12*, 2798–2809. [CrossRef]

17. Khan, M.A.; Alothman, Z.A.; Naushad, M.; Khan, M.R.; Luqman, M. Adsorption of methylene blue on strongly basic anion exchange resin (Zerolit DMF): Kinetic, isotherm, and thermodynamic studies. *Desalination Water Treat.* **2015**, *53*, 515–523. [CrossRef]
18. Ganiyu, S.O.; dos Santos, E.V.; Costa, E.C.T.d.A.; Martínez-Huitle, C.A. Electrochemical advanced oxidation processes (EAOPs) as alternative treatment techniques for carwash wastewater reclamation. *Chemosphere* **2018**, *211*, 998–1006. [CrossRef]
19. Tagliavini, M.; Schäfer, A.I. Removal of steroid micropollutants by polymer-based spherical activated carbon (PBSAC) assisted membrane filtration. *J. Hazard. Mater.* **2018**, *353*, 514–521. [CrossRef] [PubMed]
20. Olusegun, S.J.; Freitas, E.T.F.; Lara, L.R.S.; Stumpf, H.O.; Mohallem, N.D.S. Effect of drying process and calcination on the structural and magnetic properties of cobalt ferrite. *Ceram. Int.* **2019**, *45*, 8734–8743. [CrossRef]
21. Ramlow, H.; Machado, R.A.F.; Bierhalz, A.C.K.; Marangoni, C. Dye synthetic solution treatment by direct contact membrane distillation using commercial membranes. *Environ. Technol.* **2020**, *41*, 2253–2265. [CrossRef]
22. Okoli, C.P.; Ofomaja, A.E. Development of sustainable magnetic polyurethane polymer nanocomposite for abatement of tetracycline antibiotics aqueous pollution: Response surface methodology and adsorption dynamics. *J. Clean. Prod.* **2019**, *217*, 42–55. [CrossRef]
23. Li, X.-D.; Zhai, Q.-Z. Use of nanometer mesoporous MCM-41 for the removal of Pb(II) from aqueous solution. *Appl. Water Sci.* **2020**, *10*, 1–10. [CrossRef]
24. Qin, X.; Liu, F.; Wang, G.; Weng, L.; Li, L. Adsorption of levofloxacin onto goethite: Effects of pH, calcium and phosphate. *Colloids Surf. B Biointerfaces* **2014**, *116*, 591–596. [CrossRef]
25. Baran, W.; Adamek, E.; Jajko, M.; Sobczak, A. Removal of veterinary antibiotics from wastewater by electrocoagulation. *Chemosphere* **2018**, *194*, 381–389. [CrossRef]
26. Sun, J.; Cui, L.; Gao, Y.; He, Y.; Liu, H.; Huang, Z. Environmental application of magnetic cellulose derived from Pennisetum sinese Roxb for efficient tetracycline removal. *Carbohydr. Polym.* **2021**, *251*, 117004. [CrossRef]
27. Zhou, J.; Wu, P.; Dang, Z.; Zhu, N.; Li, P.; Wu, J.; Wang, X. Polymeric Fe/Zr pillared montmorillonite for the removal of Cr(VI) from aqueous solutions. *Chem. Eng. J.* **2010**, *162*, 1035–1044. [CrossRef]
28. Vargas, A.M.M.; Cazetta, A.L.; Kunita, M.H.; Silva, T.L.; Almeida, V.C. Adsorption of methylene blue on activated carbon produced from flamboyant pods (Delonix regia): Study of adsorption isotherms and kinetic models. *Chem. Eng. J.* **2011**, *168*, 722–730. [CrossRef]
29. Zhang, D.; Yin, J.; Zhao, J.; Zhu, H.; Wang, C. Adsorption and removal of tetracycline from water by petroleum coke-derived highly porous activated carbon. *J. Environ. Chem. Eng.* **2015**, *3*, 1504–1512. [CrossRef]
30. Brigante, M.; Avena, M. Biotemplated synthesis of mesoporous silica for doxycycline removal. Effect of pH, temperature, ionic strength and Ca^{2+} concentration on the adsorption behaviour. *Microporous Mesoporous Mater.* **2016**, *225*, 534–542. [CrossRef]
31. Lagaly, G.; Ogawa, M.; Dékány, I. Chapter 7.3 Clay Mineral Organic Interactions. *Dev. Clay Sci.* **2006**, *1*, 309–377.
32. Zhao, Y.; Cao, B.; Lin, Z.; Su, X. Synthesis of $CoFe_2O_4$/C nano-catalyst with excellent performance by molten salt method and its application in 4-nitrophenol reduction. *Environ. Pollut.* **2019**, *254*, 112961. [CrossRef] [PubMed]